1. Vuko, VUKČEVIĆ, Faculty of Mechanical Engineering and Naval Architecture, University of Zagreb, Ivana Lučića 5, vuko.vukcevic@fsb.hr *(corresponding author)*
2. Borna, ŠOJAT, Faculty of Mechanical Engineering and Naval Architecture, University of Zagreb, Ivana Lučića 5, bornaa.sojat@gmail.com
3. Inno, GATIN, Faculty of Mechanical Engineering and Naval Architecture, University of Zagreb, Ivana Lučića 5, innogatin@gmail.com
4. Hrvoje, JASAK, Faculty of Mechanical Engineering and Naval Architecture, University of Zagreb, Ivana Lučića 5, hrvoje.jasak@fsb.hr

VALIDACIJA I VERIFIKACIJA PRORAČUNA POMORSTVENOSTI BRODA POMOĆU PROGRAMA OPENFOAM

Sažetak

U ovom radu je prikazana detaljna studija validacije i verifikacije proračuna pomorstvenosti broda pomoću programa računalne dinamike fluida OpenFOAM. Za jedrilicu DSYHS #44, različiti valovi u pramac pri konstantnom Froude-ovom broju su simulirani te su rezultati uspoređeni s eksperimentalnim podatcima. Za kontejnerski brod "KRISO Container Ship" (KCS), provedene su simulacije za velik broj slučajeva nailaznog vala, pri projektnom Froude-ovom broju. Varirane su karakteristike valova i kut nailaska vala u odnosu na smjer napredovanja broda. Rezultati otpora broda na valovima, poniranja, posrtanja i ljuljanja uspoređeni su s eksperimentalnim podatcima. Sve simulacije provedene su na tri proračunske mreže kako bi se provela analiza osjetljivosti rješenja na rezoluciju mreže.

Ključne riječi na hrvatskom: otpor broda na valovima, pomorstvenost broda, računalna dinamika fluida, OpenFOAM.

VALIDATION AND VERIFICATION OF SEAKEEPING IN OPENFOAM

Abstract

In this paper a detailed validation and verification of seakeeping simulations using Computational Fluid Dynamics (CFD) software OpenFOAM is presented. For the DSYHS #44 sailing boat, different head wave conditions for a fixed Froude number are simulated and the results are compared to experimental data. For the KRISO Container Ship (KCS), a large number of incident wave cases is considered at design Froude number. Incident wave parameters and direction of wave propagation with respect to ship's heading are varied. The results for the total resistance, heave, pitch and roll are compared to experimental data. All simulations are conducted on three different grids in order to assess numerical uncertainties.

Key words in English: Ship Resistance in Waves, Seakeeping, Computational Fluid Dynamics, OpenFOAM.

1. Introduction

Seakeeping simulations are traditionally carried out with potential flow methods, which have been successfully used as a reliable tool for more than two decades. However, certain disadvantages of the potential flow model (inviscid, irrotational, single-phase flow) and its difficulty with treatment of the forward speed, render the methods inaccurate for predictions of the added resistance in waves. Consequently, Reynolds Averaged Navier-Stokes (RANS) based CFD methods are becoming the focus of research in modern naval hydrodynamics due to:

- Immense increase in computer resources during past few decades,
- Development of highly parallel computer stations using distributed or shared memory,
- Recent regulations regarding energy efficiency and safety of ships.

A large portion of practical CFD applications encompasses seakeeping simulations, which is demonstrated by the global effort at the Tokyo 2015 Workshop to validate different CFD algorithms for head and oblique wave conditions [1]. Number of submissions for the head waves cases is significantly larger than the number of submissions for the oblique wave cases, indicating the difficulty of modelling ship's response to oblique waves [2]. The same trend can be observed in scientific journal publications regarding seakeeping CFD simulations. Carrica et al. [3] studied the behaviour of a self-propelled ship in regular head waves. Casteglione et al. [4] performed a seakeeping study of a catamaran at large Froude number in head waves. Guo et al. [5] investigated the KVLCC2 model in head waves, comparing the results with potential flow theory. Recently, Tezdogan et al. [6] investigated the seakeeping response of a slow steaming KCS in head waves. The research suggests that there is a significant difference between simulating head and oblique waves in CFD, which is often related to difficulties due to wave propagation and reflection.

In this work, we will briefly present the mathematical framework that enables efficient and non-reflective wave propagation in CFD domain. We shall discuss the two CFD solution algorithms used in this paper, which are implemented in the Naval Hydro pack and are based on Volume-of-Fluid (VOF) and Level Set (LS) methodology for interface capturing. The VOF model is used to simulate a sailing boat in head waves, where the added resistance is compared to experimental data. Both models are then used to calculate the seakeeping response of two KCS models in head and oblique waves, comparing the results with experimental data. Grid uncertainties and periodic uncertainties via moving window FFT are carried out for all KCS test cases.

2. Mathematical and numerical modelling

Two CFD algorithms (solvers) are used in this study:

1. `navalFoam`: VOF based two-phase solver with domain decomposition via implicit relaxation zones [7],
2. `swenseFoam`: LS based two-phase solver with solution decomposition via SWENSE (Spectral Wave Explicit Navier-Stokes Equations) approach and domain decomposition via implicit relaxation zones [8].

Both solvers rely on embedded free surface approach [7] where the jump conditions at the free surface are used to derive interface-corrected interpolation schemes for arbitrary polyhedral cells near the free surface. The approach ensures infinitesimally sharp jump of dynamic pressure and density in numerical simulations, without loss of robustness and numerical stability.

The implicitly redistanced LS method in `swenseFoam` maintains the signed distance profile of the LS field during the transport equation, rendering additional redistacing step unnecessary.

Relaxation zones are used to prevent wave reflection off the farfield boundaries in both solvers. Inside relaxation zones, fully non-linear, two-phase, turbulent CFD solution is gradually blended towards the desired potential flow solution, preventing undesirable wave reflection. Since the solution is decomposed in `swenseFoam` into incident and perturbation components, the perturbation components are damped towards zero in the relaxation zones, leaving incident potential flow solution. The implicit treatment of relaxation zones in both `navalFoam` and `swenseFoam` are described in detail in [7] and [8], respectively.

$k - \omega$ *SST* two-equation eddy viscosity turbulence model is used in this paper.

Coupling of the six-degrees-of-freedom (6DOF) solver with the fluid flow is resolved in outer loop at each time step. Usually, 7 outer correction steps are employed to converge the two-phase fluid flow and the 6DOF solution. Although there is a possibility of employing algebraic mesh deformation, the mesh motion is moved as a rigid body for efficiency.

3. Sailing boat DSYHS #44 validation

Delft Systematic Yacht Hull Series DSYHS #44 [9] sailing boat has been considered as a first test case for seakeeping in head waves. The Froude number of 0.325 is considered, where the particulars of the model are given in Tab. 1: length between perpendiculars, breadth, draft, mass, pitch radius of gyration, vertical and longitudinal centres of gravity, respectively. The coordinate system is right handed, with positive x-axis defined towards the bow and the positive z-axis is defined upwards. The origin of the coordinate system is located in the symmetry plane at the aft perpendicular, at the base line. The model is free to heave and pitch, with other degrees of freedom constrained. It is important to note that the experimental reports [9, 10] did not include the actual position of VCG, thus, VCG is positioned at still water line in CFD computations.

Table 1 DSYHS #44 model particulars

Tablica 1. Karakteristike DSYHS #44 modela

L_{pp}, m	B, m	T, m	m, kg	r_y, m	VCG, m	LCG, m
1.710	0.515	0.117	40.6	0.422	0.117	0.800

The dominantly hexahedral unstructured grid consists of approximately 1 850 000 cells. The average non-orthogonality is 6.5°, with maximum non-orthogonality of 82.3°. Maximum cell aspect ratio is approximately 57. Side and top view of the grid can be seen Fig. 1 and 2, respectively, where near hull and Kelvin angle refinements are visible.

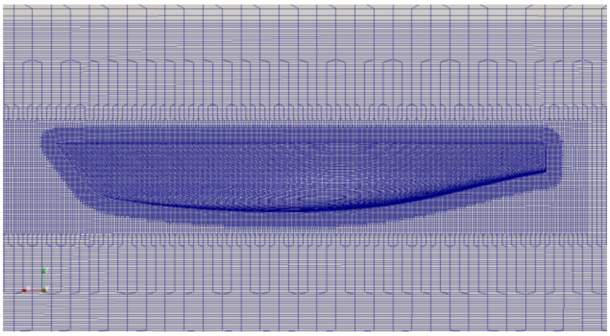

Fig. 1 Side view of the DSYHS #44 grid

Slika 1. Bočni pogled DSYHS #44 mreže

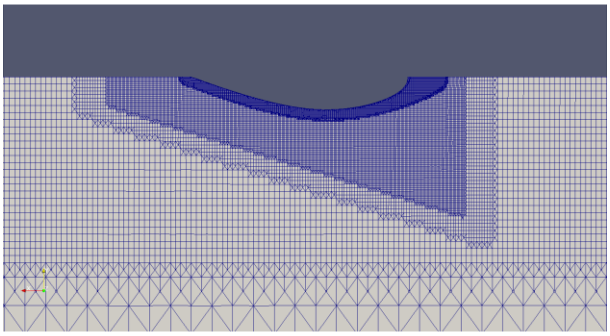

Fig. 2 Top view of the DSYHS #44 grid

Slika 2. Pogled iz ptičje perspektive DSYHS #44 mreže

The experimental measurements reported mean value of the total resistance in waves R_{TW}. Results are presented in dimensionless form following [10] by normalising with $\rho g L_{PP} \zeta_a^2$ where ρ is the water density, g is the gravitational acceleration and ζ_a is the wave amplitude.

Fig. 3 presents the steady resistance for 5 Froude numbers, where the agreement with experimental data is good for first three cases, while the discrepancy between CFD and experiments is higher for high Froude numbers. This is expected as the VCG in the experimental setup was not reported and the VCG affects trim angle of the sailboat at such large Froude numbers, thus affecting the resistance. Five head wave cases simulated with the `navalFoam` solver are reported in Tab. 2. The mean value of the total resistance is presented in Fig. 4 where it can be seen that the CFD results agree well with the experimental measurements for all cases. CFD result for the total resistance at the $\lambda/L_{PP} = 1.45$ under predicts the experimental measurements by approximately 11%, Tab. 2. Absolute values of relative errors for other cases range from 1.3% to 8%.

Table 2 Simulated conditions and relative error compared to experiments

Tablica 2. Relativna greška u odnosu ne eksperiment za zadane parametre vala

λ/L_{PP}	2.93	2.05	1.75	1.45	1.01
ζ_a m	0.0834	0.0584	0.0499	0.0413	0.0288
$(R_{TW,\,EXP} - R_{TW,\,CFD})/R_{TW,\,EXP}$, %	-5.0	1.3	7.9	10.7	4.0

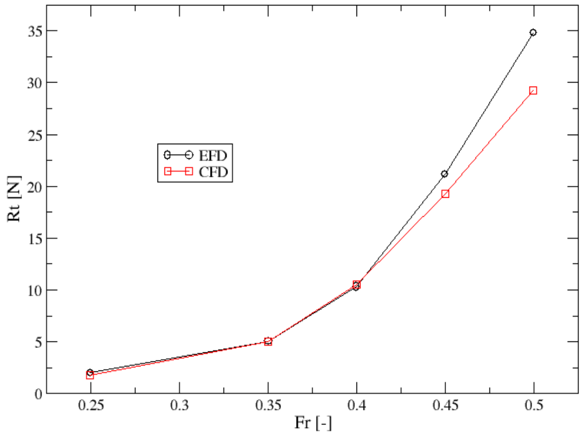

Fig. 3 Steady resistance comparison

Slika 3. Usporedba otpora na mirnoj vodi

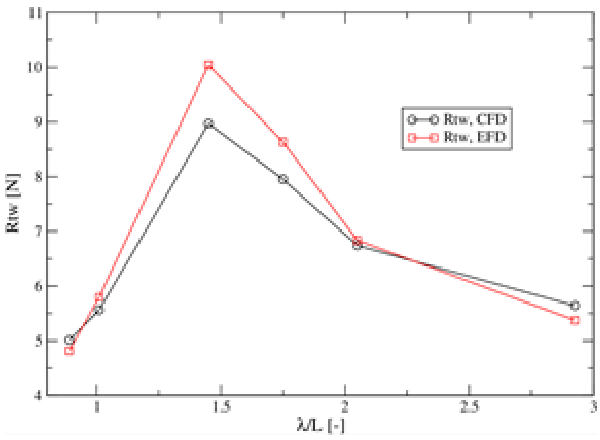

Fig. 4 Mean total resistance in waves comparison

Slika 4. Usporedba srednje vrijednosti otpora na valovima

4. KCS head waves validation and verification

Latest experimental results and detailed instructions for the KCS model tests can be found at the Tokyo 2015 workshop's website [1]. Case set 2.10 comprises 5 head wave cases: C1, C2, C3, C4 and C5 (C1 representing the shortest wave length and smallest wave height). Only the design Froude number of 0.26 is considered, and the model is towed in free heave and pitch conditions. Heave, pitch and the total resistance coefficient are measured, but the experimental uncertainty has not been assessed.

Three unstructured grids with a symmetry plane are used with approximately: 600 000, 950 000, 1 600 000 cells. Compared to other participants [2], our grids are an order of magnitude smaller and no topology conforming grids have been created for each specific test case, which is usually done to preserve number of cells per wave height and wave length; instead the three grids have been used for all wave parameters.

Measured items exhibit a combination of monotone and oscillatory convergence with particular items diverging (usually higher order motion harmonics). The grid uncertainty is assessed following Simonsen et al. [11]. The time domain signals are processed via moving window FFT with a square window corresponding to the encounter period. Periodic convergence for all measured items is observed to be oscillatory, stabilising after approximately 20 periods. The corresponding periodic convergence is calculated using guidelines by Stern et al. [12] for oscillatory convergence.

Results are presented in terms of dimensionless Response Amplitude Operators (RAOs) in Fig. 5, Fig. 6 and Fig. 7 for different dimensionless wave lengths (normalised with length between perpendiculars). The red line denotes the first order harmonic amplitude, while the black line denotes the mean value. Experimental results are denoted with dashed lines, while the `navalFoam` and swenseFoam results are denoted with dotted and solid lines, respectively.

First order harmonic amplitudes of heave and pitch motions are in good agreement with experimental data. For higher wave lengths (and consequently wave heights, following the experimental setup), `navalFoam` under predicts the motion amplitude compared to experimental and `swenseFoam` results. Mean values of heave and pitch motions are in good agreement with experimental data, except for the mean value of heave calculated with `swenseFoam`, which seems to be offset by a constant value for all wave lengths. Mean value of the total resistance coefficient calculated by `navalFoam` is in better agreement with experimental data compared to `swenseFoam`. `swenseFoam` over predicts the mean value of resistance for all wave lengths, which we believe to be related to a software bug in the specific dissipation rate equation in the turbulence model. The software bug has been corrected for all other simulations (sailing yacht, head waves KCS with `navalFoam` and oblique waves KCS). The first order harmonic amplitude of the total resistance coefficient calculated by both solvers is in good agreement with experimental data, where `navalFoam` under predicts experimental and `swenseFoam` results.

Fig. 8 shows periodic convergence of the mean value total resistance coefficient for the C5 case, via moving window FFT with a square window corresponding to the encounter period. Both `navalFoam` and `swenseFoam` exhibit similar convergence trend. Periodic uncertainties for mean value and first order are lower than 2%, which has been achieved by simulating at least 20 encounter periods.

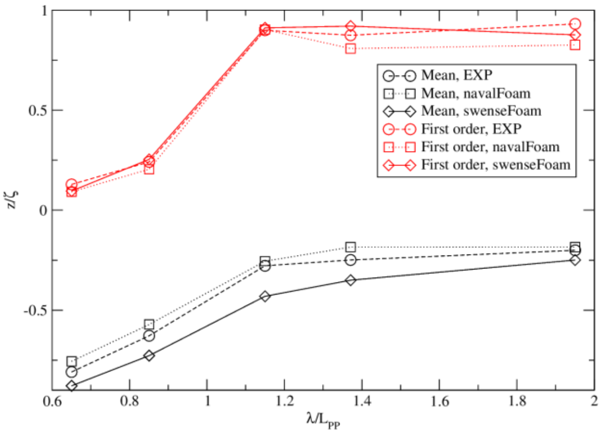

Fig. 5 Heave RAO, head waves KCS

Slika 5. RAO poniranja, valovi u pramac KCS

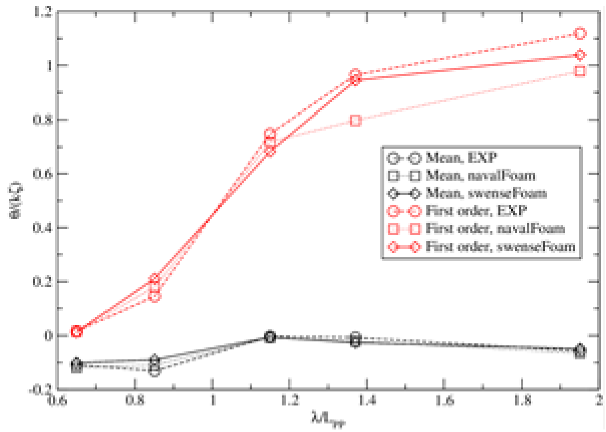

Fig. 6 Pitch RAO, head waves KCS

Slika 6. RAO posrtanja, valovi u pramac KCS

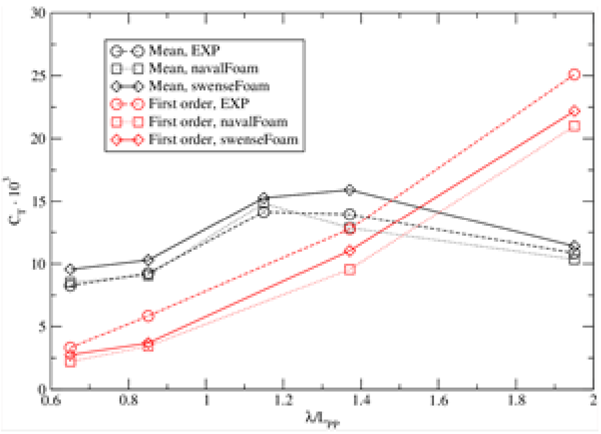

Fig. 7 Resistance coefficient RAO, head waves KCS

Slika 7. RAO koeficijenta otpora, valovi u pramac KCS

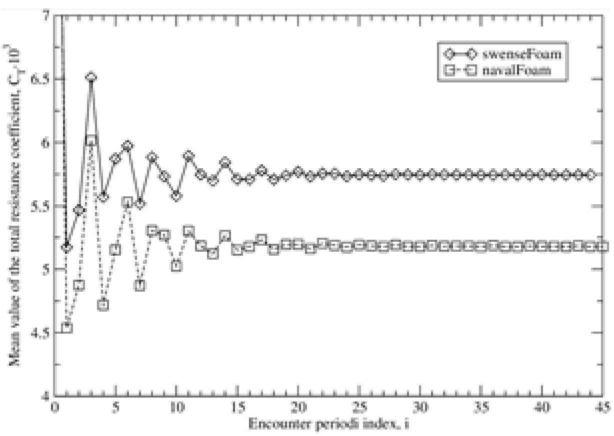

Fig. 8 Periodic convergence example

Slika 8. Primjer periodične konvergencije

Average uncertainty for the mean value of the total resistance coefficient is 3.3% for five cases. First order harmonic uncertainties for the total resistance coefficient is less than 2%, except for the resonant C3 case with uncertainty of 12.5%. Grid uncertainties for first order harmonic amplitude of heave and pitch are generally lower than 2%. Reader is referred to [7] for a more detailed review of grid uncertainties.

As a representative example, CPU time for the simulation of the resonant C3 case with `swenseFoam`, on a grid with 1.6 million cells took 50 minutes per encounter period on 40 3.5 GHz cores. Approximately 300 time-steps have been used per encounter period, simulating the total of 30 encounter periods in order to ensure proper periodic convergence.

5. KCS oblique waves validation and verification

Case set 2.11 of the Tokyo 2015 workshop [1] comprises 5 oblique wave cases: C1 (head waves, 0º), C2 (bow waves, 45º), C3 (beam waves, 90º), C4 (quartering waves, 135º) and C5 (following waves, 180º). The experimental measurements report heave, roll and pitch motions and total resistance coefficient. During experiments, the model was restrained using a spring system, which we assume has impaired the quality of experimental measurements at least for first order response of the resistance.

The three grids in the head waves study are mirrored with respect to the symmetry plane, producing grids with a doubled cell count. It is important to note that the finest grid with approximately 3 million cells is an order of magnitude smaller than the grid used by other participant. Compared to approximately ten submissions for the head waves cases (2.10), only two groups submitted the results for oblique waves (2.11): CFDShip-Iowa and us (University of Zagreb, using `swenseFoam` solver).

As in the head waves cases, measured items exhibit a combination of monotone and oscillatory convergence with a small number of diverging items. The grid uncertainty is assessed following Simonsen et al. [11], and the periodic uncertainty is assessed as in the head waves case.

Fig. 9, 10, 11 and 12 represent RAOs of mean, first and second order harmonic amplitude for different encounter angles. First order amplitude of heave (Fig. 9) agrees well with experimental data for all encounter angles. Small second order amplitude of heave is captured reasonably well with CFD, with the exception of quartering waves (135º) where a second order response larger than the first order has been measured in experiments. Mean value of heave motion compares well with experimental data, except for the beam and quartering waves where experiments report positive values. First order amplitude of pitch (Fig. 10) agrees well with experimental data with the largest discrepancy for quartering waves. Small second order amplitude of pitch is reasonably well captured compared to experiments. Mean value of pitch motion has the opposite sign in experimental measurements, which we believe to be related to different post processing convention used for experiments. First order amplitude of roll (Fig. 11) also agrees well with experimental data, except for the beam waves case where the experiments report first order amplitude of the same order as in the following waves. Although the parametric roll should not occur for this model, significant mean values of roll have been measured in experiments for head and following waves, whereas CFD response is negligibly small.

The largest discrepancy compared with experimental data is the first order amplitude of the total resistance coefficient, which has 1 to 2 orders of magnitude smaller values. We believe that such unreasonably low values are related to experimental setup with a spring system. Mean value of the added resistance compares well with the experimental data for head and bow waves, with larger discrepancies for beam, quartering and following waves. It is also worthy to note that the experimentally measured mean value of total resistance coefficient for beam waves was smaller than the resistance coefficient in calm water (for the same Froude number and model).

Periodic uncertainties for mean and first order amplitudes of all measured items (heave, roll, pitch and total resistance) are below 1% of the finest grid results. This is ensured by simulating a large number of encounter periods, e.g. up to 70 for quartering waves.

Grid uncertainties for the mean value of the total resistance coefficient are approximately 10% on average for all headings. The first order amplitudes have grid uncertainties lower than 3%, except for the beam waves (C3) case with a high grid uncertainty of approximately 59%. The reason for high uncertainty is minor influence of the beam waves on the total resistance of a ship. Grid uncertainties for the mean value of heave motion range from 2% for head waves (C1) to 27% for quartering waves, which is the most demanding condition with large motion amplitudes. First order harmonic amplitudes of heave have grid uncertainties smaller than 2%, except for the following waves case with grid uncertainty of 18%. Grid uncertainties for the mean value of roll are: 3% for bow waves, 7% for quartering waves and 63% for beam waves, which needs further investigation. The average grid uncertainty for the first order of the roll motion is approximately 4%. The first order harmonic amplitudes of pitch motion have grid uncertainties below 2%, except for the beam waves case with a very small pitch response.

Simulation of bow waves case took approximately 40 minutes per encounter period for a grid with 3.2 million cells on 56 3.5 GHz cores. Approximately 225 time-steps per encounter period have been used and 60 encounter periods have been simulated in total.

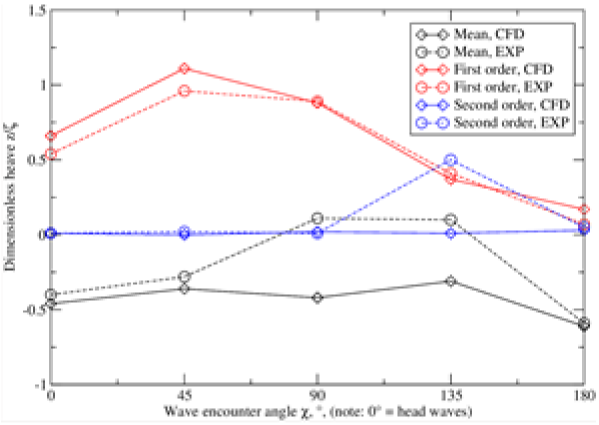

Fig. 9 Heave RAO, oblique waves KCS

Slika 9. RAO poniranja, kosi valovi KCS

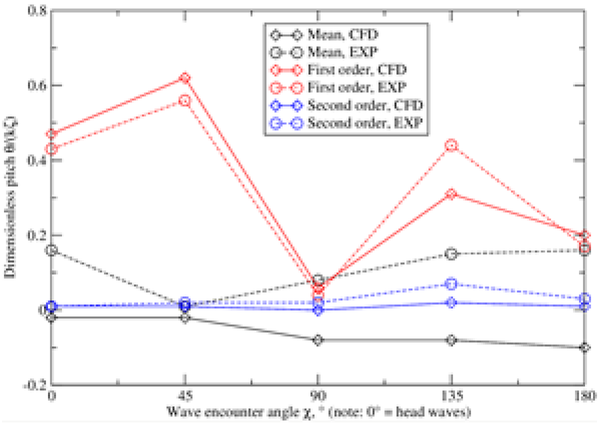

Fig. 10 Pitch RAO, oblique waves KCS

Slika 10. RAO posrtanja, kosi valovi KCS

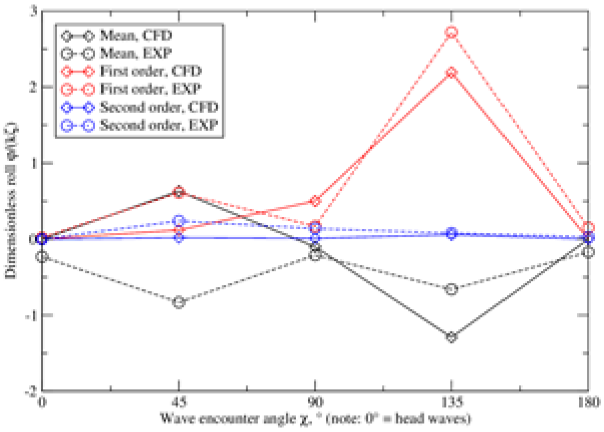

Fig. 11 Roll RAO, oblique waves KCS

Slika 11. RAO ljuljanja, kosi valovi KCS

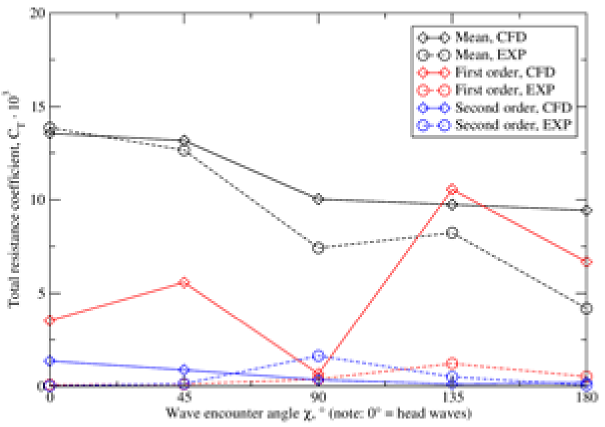

Fig. 12 Resistance coefficient RAO, oblique waves KCS

Slika 12. RAO koeficijenta otpora, kosi valovi KCS

6. Conclusion

The paper presents overview of the CFD validation and verification for seakeeping applications. CFD results obtained with two solvers: `navalFoam` (Volume-of-Fluid, without solution decomposition) and `swenseFoam` (Level Set, with solution decomposition) are compared with available experimental data.

CFD results for the sailing yacht DSYHS #44 and the KCS model agree well with the experimental data. It is important to note that the experimental measurements did not include the uncertainty assessment. A thorough grid and periodic uncertainty assessment for the KCS model in head and oblique waves has been performed. It has been demonstrated that the periodic uncertainty can be lowered by simulating more than 20 encounter periods. Grid uncertainties for the mean and first harmonic amplitudes are acceptably low for industrial applications. Along with a relatively short CPU times of approximately 40 minutes per encounter period, CFD simulations may be regarded as a reliable and cost efficient tool for seakeeping calculations.

The list of references:

[1] ...: „Tokyo 2015: A Workshop on CFD in Ship Hydrodynamics“. [Online] Available at http://www.t2015.nmri.go.jo/, 27 February 2016.

[2] LARSSON, L., STERN, F., VISONNEAU, M., HIRATA, N., HINO, T., KIM, J.: „Tokyo 2015: A Workshop on CFD in Ship Hydrodynamics, Proceedings, Volume II“, 2015.

[3] CARRICA, P. M., FU, H., STERN, F.: „Computations of self-propulsion free to sink and trim and of motions in head waves of the KRISO container ship (KCS) model“, Applied Ocean Research 33(2011)4, p. 309-320.

[4] CASTIGLIONE, T., STERN, F., BOVA, S., KANDASAMY, M.: „Numerical investigation of the seakeeping behavior of catamaran advancing in regular head waves“, Ocean Engineering 38(2011)16, p. 1806-1822.

[5] GUO, B. J., STEEN, S., DENG, G. B.: „Seakeeping prediction of KVLCC2 in head waves with RANS“, Applied Ocean Research 35(2012), p. 56-67.

[6] TEZDOGAN, T., DEMIREL, Y. K., KELLET, P., KHORASANCHI, M., INCECIK, A., TURAN, O.: „Full-scale unsteady RANS CFD simulations of ship behaviour and performance in head seas due to slow steaming“, Ocean Engineering 97(2015), p. 186-206.

[7] VUKČEVIĆ, V., JASAK, H.: „Seakeeping sensitivity studies using the decomposition CFD model based on Ghost Fluid Method“, Proceedings of 31st Symposium of Naval Hydrodynamics, Monterey, California, 2016. Accepted for publication.

[8] VUKČEVIĆ, V., JASAK, H.: „Seakeeping Validation and Verification Using Decomposition Model Based on Embedded Free Surface Method“, Proceedings of the Tokyo 2015: A Workshop on CFD in Ship Hydrodynamics, NMRI, 2015, p. 437-442.

[9] KEUNING, J. A., ONNINK, R., DAMMAN, A.: „The Influence of the Bowshape on the Performance of a Sailing Yacht“, Proceedings of 16th International HISWA Symposium on Yacht Design and Yacht Construction, 2000, Report 1238-P, p. 107-122.

[10] KEUNING, J. A., VERMEULEN, K. J., TEN HAVE, H. P.: „An Approximation Method for the Added Resistance in Waves of a Sailing Yacht“, Proceedings of 2nd International Symposium on Design and Production of Motor Sailing Yachts, MDY'06, Madrid, 2016.

[11] SIMONSEN, C. D., OTZEN, J. F., JONCQUEY, S., STERN, F.: „EFD and CFD for KCS heaving and pitching in regular head waves“, Journal of Marine Science and Technology 18(2013), p. 435-459.

[12] STERN, F., WILSON, R.V., COLEMAN, H. W., PATERSON, E. G.: „Comprehensive Approach to Verification and Validation of CFD Simulations-Part 1: Methodology and Procedures“, Journal of Fluid Engineering 123(2001)4, p. 793-802.